Impurity induced low-energy resonances in $Bi_2Sr_2CaCu_2O_{8+\delta}$

Jian-Ming Tang and Michael E. Flatté
Department of Physics and Astronomy, University of Iowa, Iowa City, Iowa 52242-1479

We study sharp low-energy resonance peaks in the local density of states (LDOS) induced by Zn impurities or possible Cu vacancies in superconducting $Bi_2Sr_2CaCu_2O_{8+\delta}$. The measured structure of these near-zero-bias resonances is quantitatively reproduced by an extended impurity potential without invoking internal impurity states or sophisticated tunneling models. The Zn potential extends at least to the nearest-neighbor Cu sites, and the range of order parameter suppression extends at least 8 Å away from the Zn site. We further show that the local spin susceptibilities near Zn impurities increase rather than decrease with decreasing temperature in the superconducting state due to the sharp increase of LDOS near the Fermi level.

PACS numbers: 74.62.Dh,74.25.Jb,74.20.Rp,74.72.Hs

Recent scanning tunneling microscopy (STM) measurements on the high-T_c superconductor $Bi_2Sr_2CaCu_2O_{8+\delta}$ (BSCCO) have revealed the detailed spectral and spatial structures of sharp resonances inside the superconducting gap induced by the impurities Zn[1] and Ni[2], and by defects such as Cu vacancies.[3] The properties of these resonances depend on interactions at the atomic scale between impurity potentials and the coherent superconducting state. As work progresses to probe these defects in the underdoped regime, and above T_c, it is essential to understand whether the properties in the superconducting state can be understood within d-wave BCS theory, or whether vestiges remain of the exotic correlated state present at higher temperatures.[4,5,6,7] Detailed theoretical studies have shown that the resonances induced by a Ni impurity in BSCCO can be well described by Bogoliubov quasiparticles scattering off a potential in a d-wave superconductor with a small, but discernible, local order parameter suppression.[8] On the other hand, theories based on pointlike potentials have failed to explain quantitatively both the spatial structure of the resonances and the equally important information yielded by the spatial structure of the "coherence peaks", either for Zn impurities or Cu vacancies.[4,5,6,7]

Zn impurities induce a sharp resonance at an energy close to the Fermi level. Experimental results show that these resonances possess a large spectral weight of local density of states (LDOS) at the impurity site, whereas theories based on pointlike potentials predict that the spectral weight at the impurity site is strongly suppressed by the unrealistically large strength of the potential. This discrepancy in the spatial structure has led to various proposals. Some suggest the need for strongly correlated models, in which the internal states of the impurity are important,[5,6] and others suggest that the spatial structure measured by STM is filtered by the surface Bi-O layer above the Cu-O planes.[6,7] However, none of these proposals has provided a coherent quantitative account for the STM spectra, at both the resonance and the coherence peaks, for both Zn and Ni impurities. In this Letter, we show that the effects of Zn impurities over the entire spectrum can be quantitatively described by spatially extended potentials, and, therefore, render the potential model a fully quantitative description for both Zn and Ni impurities in BSCCO. A principal, and unexpected, conclusion is that the potentials required to model the Zn impurity are nonmagnetic and relatively weak (< 100 meV), comparable in strength to the potentials induced by the Ni impurity. Another important result is that the order parameter suppression near Zn is much more extensive than for Ni. We further report that the Cu vacancy[3] is well described within such a potential model, thus demonstrating that the potential model works for all three known defects probed by STM in BSCCO.

The appearance of near-zero-bias resonances is intrinsically important because they greatly influence the bulk response to external fields, such as conductivity and spin susceptibility. Here we also calculate the local spin susceptibilities near a Zn impurity. In the homogeneous bulk superconducting state, the spin susceptibility decreases with decreasing temperature due to the opening of a gap in LDOS around the Fermi level. However, in the presence of a sharp near-zero-bias resonance, the local spin susceptibilities near the impurity increase with decreasing temperature, and eventually the values peak at a low temperature scale set by the resonance energy. In other words, above this temperature scale, the local spin susceptibilities inversely scale with temperature, similar to the Curie behavior of a paramagnetic ion in an insulator. We find such behavior describes the Knight shifts on and near Zn in BSCCO.

We begin by describing the nature of the spatially-extended potential that quantitatively describes all of the local spectra near the Zn impurity (shown in Fig. 1). The failure of a pointlike potential to induce the correct spatial structure of Zn's near-zero-bias resonance originates from the large value of the potential (> 1 eV) required to draw states deep into the center of the gap. The strong on-site potential diminishes the spectral weight of the LDOS at the impurity site, and moves the largest spectral weights to the four nearest-neighbor sites. Experimentally the largest spectral weights, in order from largest to smallest, are at the impurity site, at the second-nearest-neighbor sites, and then at the third-nearest-

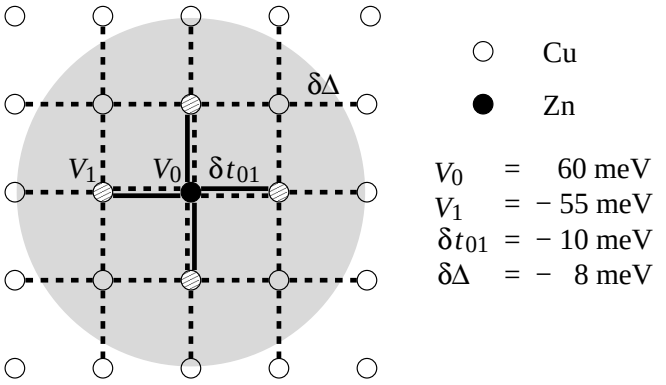

FIG. 1: A schematic diagram showing the proposed model of a Zn impurity on the Cu–O plane. Parameters extracted from fitting to the data are listed on the right. The superconducting order parameters on the dashed links are completely suppressed. This model also works for the Cu vacancy with $V_0 = 110$ meV, $V_1 = -50$ meV, and $\delta t_{01} = 19$ meV. For the Cu vacancy the order parameter was suppressed to zero ($\delta\Delta_{ij} = -\Delta_{ij}$) within 8 Å of the vacancy, and by 70% ($\delta\Delta_{ij} = -0.7\Delta_{ij}$) from 8 Å to 12 Å from the vacancy.

neighbor sites (See Figs. 2 and 3). Such a structure is consistent with a non-zero potential at the four nearest-neighbor sites. A key feature is that the potential at the impurity site is of the opposite sign to those at the nearest-neighbor sites, consistent with the structure of a screened charge perturbation. The presence of a non-magnetic spatially extended potential and a short-ranged charge oscillation is consistent also with the results of nuclear quadruple resonance (NQR) measurements on Zn impurities in $YBa_2Cu_4O_8$ (YBCO).[9] These potentials at the nearest-neighbor sites are much more effective than merely an on-site potential in inducing a sharp resonance close to the Fermi level. Unrealistically large values for the potential are no longer required. A moderate-range local suppression of the order parameter also further drives the resonance energy toward the Fermi level.[8,10] Thus a quantitative understanding of the experimental data requires careful consideration of the detailed potential structure. The same model, but with different values for the potentials, including a longer-range order parameter suppression, describes the Cu vacancy.

We use the Koster-Slater approach to calculate the LDOS around impurities.[8,11,12] Homogeneous BSCCO is modeled by a one-band tight-binding Hamiltonian, as described in Ref. 8. The Green's function of the homogeneous system is first evaluated with an energy resolution δ. The Green's function with impurities is then calculated by solving the Gorkov (Dyson) equation. The impurity potential consists of site-diagonal matrix elements at the impurity site (V_0) and at the nearest-neighbor sites (V_1), and off-diagonal matrix elements corresponding to modifications of the hopping matrix elements (δt), and of the superconducting order parameters ($\delta\Delta$) as described in Ref. 8 for the Ni impurity. The full Hamiltonian that describes the one impurity problem takes the following form,

$$\begin{aligned} H &= -\sum_{\langle i,j\rangle,\,\sigma} (t_{ij} + \delta t_{ij}) c^\dagger_{i\sigma} c_{j\sigma} \\ &\quad + \sum_{\langle i,j\rangle} \left[(\Delta_{ij} + \delta\Delta_{ij}) c^\dagger_{i\uparrow} c^\dagger_{j\downarrow} + \text{H.c.} \right] \\ &\quad + \sum_{\sigma} \left[V_0 c^\dagger_{0\sigma} c_{0\sigma} + V_1 \sum_{k=1}^{4} c^\dagger_{k\sigma} c_{k\sigma} \right] , \end{aligned} \tag{1}$$

where i and j label the lattice sites (the impurity resides at site 0), and σ labels spin. The hopping matrix elements, $t_{ij} = \{148.8, -40.9, 13, 14, -12.8\}$ meV, are based on a one-band parameterization of the angle-resolved photoemission data.[13] The superconducting order parameters, Δ_{ij}, of the homogeneous system are only non-zero on the bonds connecting two nearest-neighbor sites, $\Delta_{i,i+\hat{x}} = -\Delta_{i,i+\hat{y}} = \Delta_0/4$, where Δ_0 is the gap maximum. The momentum-dependent order parameter resulting from these Δ_{ij} has d-wave symmetry, $\Delta_{\mathbf{k}} = (\Delta_0/2)(\cos k_x L - \cos k_y L)$, where L is the lattice spacing between two Cu atoms.

To construct the effective potential for the Zn impurity, we relate important features in the LDOS data to different parts of the potential structure. First of all, it is known from STM that there is microscopic inhomogeneity of the LDOS gap, which appears to be related to the local doping concentration.[14] Judging by the experimental LDOS spectrum at a site within the same local patch as the Zn impurity, but reasonably far away from the impurity, we determine that the gap maximum Δ_0 is about 32 meV in Ref. 1. The local chemical potential μ is shifted with respect to the optimal doping value (-130.5 meV)[13] by -20 meV, which sets the Van Hove peak to be about 14 meV below the Fermi level. The energy resolution δ is about 2 meV, roughly judging by the widths of the coherence peaks and of the Zn resonance. The range of order parameter suppression is then determined by the closing in of the local gap edge. Because the amplitude of the remnant coherence peak is strongly suppressed and the appearance of mid-gap resonances contributes additional spectral weight inside the gap, our fit for the gap edge is not as quantitative as for other features of the resonance. Nevertheless, the minimum range of the order parameter suppression is determined to be about 2 lattice constants away from the impurity. That is, the order parameter is completely suppressed within a circle with a radius of approximately 8 Å. This is a much more extensive order parameter suppression than seen around the Ni impurity,[8] and suggests that Zn is more destructive to local superconductivity.

The matrix elements V_0, V_1 and δt_{01} are then determined based on the resonance energy and the peak amplitudes at three different sites (the impurity site, the 1st and the 2nd nearest-neighbor sites). Although all 3 parameters jointly determine the spatial structure, V_1 is the most dominant component. V_0 is used to obtain the correct resonance energy and δt_{01} is used to adjust the

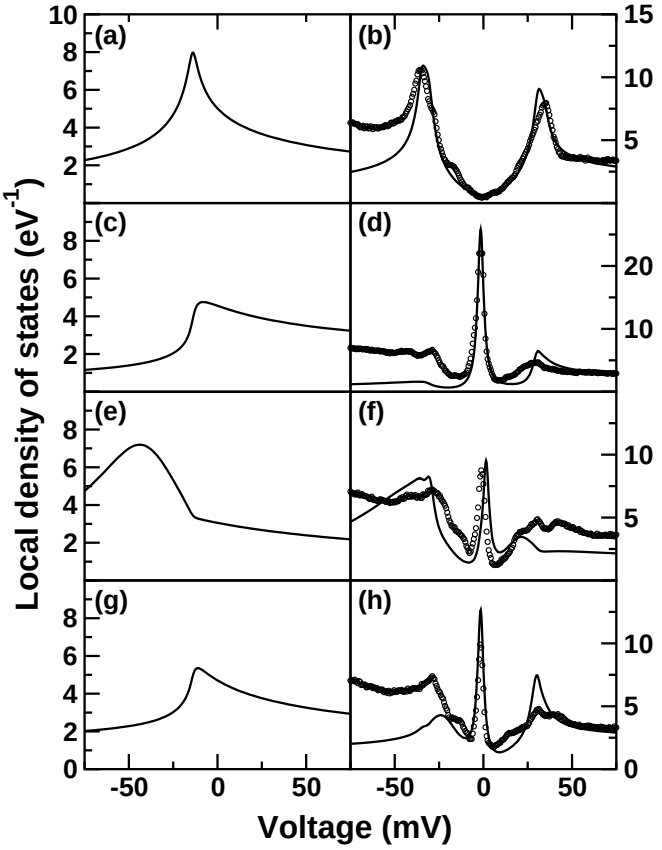

FIG. 2: LDOS spectra per unit cell at various sites near a Zn impurity. The left panels show the spectra in the "normal state" (simply setting $\Delta_{ij} = 0$) using the same impurity parameters. The right panels show the spectra in the superconducting state. Solid lines show the calculated results. (a) and (b) are the spectra at a site far away from the Zn impurity. (c) and (d) are the spectra right at the impurity site. (e) and (f) are the spectra at the 1st nearest-neighbor sites. (g) and (h) are the spectra at the 2nd nearest-neighbor sites. Open circles (○) show the STM differential conductance data.[1] The data was rescaled by a constant factor identical for all the spectra. Note that the effective potential in the "normal state" could be very different.

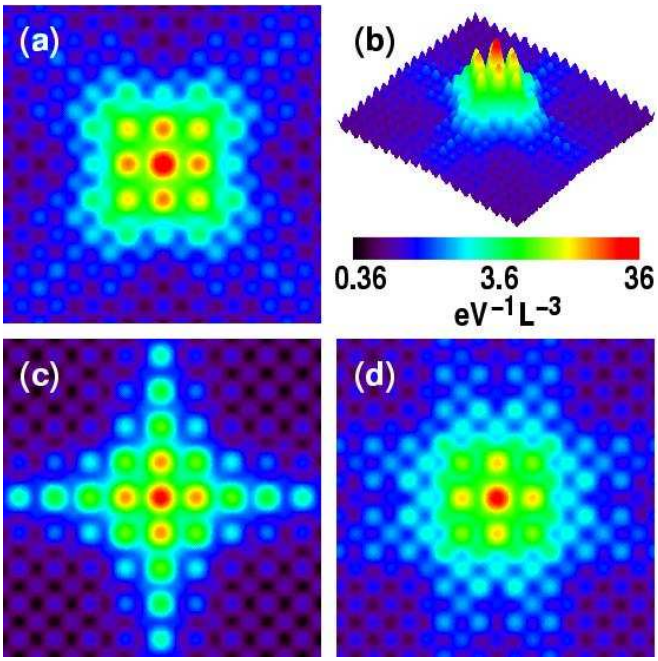

FIG. 3: (color) Spatial structure of the LDOS near a Zn impurity at -2 meV in (a) 2D and (b) 3D view. We have spatially distributed the LDOS at each unit cell according to a normalized Gaussian with a width of half the lattice spacing (L). The LDOS is shown in logarithmic scale. The Cu-O lattice is rotated by 45° so that the horizontal axis is aligned with the superlattice modulation. To demonstrate the effect of the band structure, we carried out similar calculations for tight-binding bands with (c) only the nearest-neighbor hopping ($\{t_1, \mu, V_0, V_1\} = \{150, 10, 100, -100\}$ meV) and with (d) only the nearest-neighbor and the second-nearest-neighbor hopping ($\{t_1, t_2, \mu, V_0, V_1\} = \{150, -40, -150, 75, -75\}$ meV). The chemical potential is chosen so that the Van Hove singularity is fixed at the same energy. The impurity potential is also slightly altered to keep the resonance energy at the same place.

ratio between the peaks. Our procedure provides similar spatial structures if the sign of both V_0 and V_1 are reversed – we can only determine that they have opposite sign relative to each other.[15] Motivated by the NQR experiments that suggest electron charge accumulation on the nearest-neighbor sites of Zn in YBCO, we choose the potential energy on the nearest-neighbor sites to have negative values (attractive to electrons).

Figure 2 shows the detailed comparisons of our calculations with data. In general, we have a good fit for the spectra in a wide energy range inside the gap. The fit is less satisfactory for the energy range beyond the coherence peaks. Therefore, the determination of the gap edge is not as precise as the determination of other parameters based on the resonance energy and peak spectral weights. We note that for every midgap resonance one expects a feature on the nearest-neighbor sites which is on the opposite side from that on the impurity site itself.[4,16] For these spatially-extended potentials, however, the spectral weight of these resonance peaks is highly reduced and likely not visible.

The spatial structure of the resonance peak, suitable for direct comparison with Ref. 1, is shown in Fig. 3. Note that the spectral weight is most peaked along the $(1, 1)$ direction of the Cu-O lattice in the near region around the impurity. Far from the impurity, the tails align with the Cu-O bond direction (This is also the case for Ni, but the signal is much weaker.) As our fit of the local potentials was constrained entirely by features near the impurity, obtaining good agreement with measured data for this orientation of the resonance tail suggests that we have a reasonable description of the BSCCO band structure near the Fermi level. For example, in a simple nearest-neighbor tight-binding model we find that the long-ranged tail of the resonance incorrectly follows the

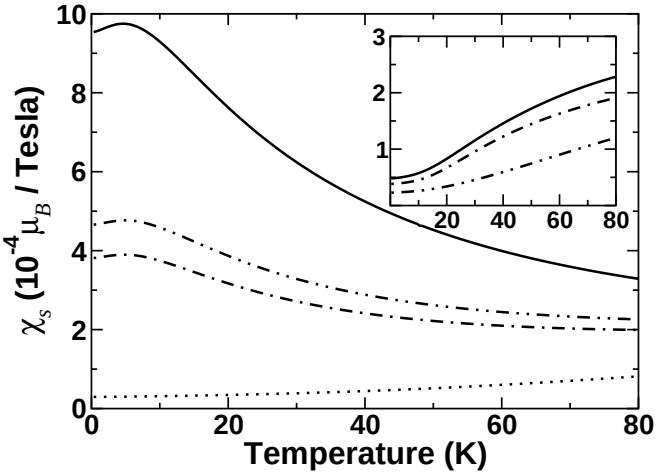

FIG. 4: The local spin susceptibilities at the Zn site (solid line), at the 1st nearest-neighbor sites (dot-dashed line), at the 2nd nearest-neighbor sites (double dot-dashed line), and at a faraway site (dotted line). The susceptibilities near Zn show a Curie-like behavior in an intermediate temperature range (above 10 K and below the superconducting transition temperature). The inset shows the corresponding susceptibilities near a Ni impurity, which simply increase with temperature.

diagonal of the Cu-O lattice [Fig. 3(c)]. The tail begins to rotate to follow correctly the Cu-O bond direction when the second-nearest-neighbor hopping is added [Fig. 3(d)], and the proper orientation is obtained in the full tight-binding model for BSCCO. We have verified that this defect model, with the different potentials reported in Fig. 1, also describes well the more limited Cu vacancy data in Ref. 3. The order parameter suppression even more extended around the Cu vacancy than around the Zn impurity; our model parameters are listed in the Fig. 1 caption.

To show that the bulk response to fields can be dramatically changed by the appearance of the near-zero-bias resonance, we calculate the local spin susceptibilities (suitable for determining the Knight shifts) around the impurity using our results for the LDOS. The local spin susceptibility at site j is defined as

$$\chi_s \;=\; \frac{\mu_B^2}{k_B T}\int d\omega A_j(\omega) f(\omega)[1-f(\omega)]\;, \qquad (2)$$

where μ_B is the Bohr magneton, k_B is the Boltzmann constant, T is temperature, $A_j(\omega)$ is the LDOS at site j, and $f(\omega)$ is the Fermi-Dirac distribution function. We assume $g = 2$. The results for both Zn and Ni impurities are shown in Fig. 4. For Zn the local spin susceptibility increases as the temperature decreases, and there is a maximum at a very low temperature, which is determined by the resonance energy. The strongest response is at the impurity site, and the signal strengths at the 1st and 2nd nearest-neighbor sites are approximately equal. Ni, which has a much higher resonance energy, does not show this low-temperature maximum, and thus does not appear to be paramagnetic in this type of experiment. Thus we find that the resonance induced by a completely nonmagnetic impurity potential for Zn generates a signal in spin susceptibility experiments that closely mimics the expected signal from a free spin (as suggested in Ref. 17). This result may have implications for measurements of spin susceptibilities in $YBa_2Ca_3O_{7-\delta}$.[18]

We have provided a reasonable nonmagnetic potential model that quantitatively reproduces the spatial structure of the Zn impurity resonance and the spatial structure of the coherence peaks near Zn. We have verified that the potential model also produces accurate results for the Cu vacancy. The model is based on the same BSCCO electronic structure as used previously to describe Ni, thus demonstrating that a consistent picture is possible that quantitatively describes all three defects in BSCCO. Surprisingly small effective potentials are required to describe the Zn resonance, even though it occurs near zero energy. The order parameter suppression we find near Zn is more extensive than near Ni, but not as extensive as near the Cu vacancy. We have also demonstrated that the resonance near Zn would respond in spin susceptibility measurements in a way that would mimic a free spin, whereas Ni would not. Finally, the potential for the vacancy, and to a lesser extent Zn, scatters quasiparticles most effectively for momentum transfer (π, π). This may broaden quasiparticle signatures significantly at the $(\pi, 0)$ points of the Brillouin zone. These results provide a foundation for better understanding of measurements that are likely to be made on these defects in the more exotic "pseudogap" state of BSCCO at higher temperatures.

We thank E. W. Hudson and J. C. Davis for providing data shown in Fig. 2. This work is supported by ONR Grant Nos. N00014-04-1-0046 and N00014-99-1-0313.

[1] S. H. Pan, E. W. Hudson, K. M. Lang, H. Eisaki, S. Uchida, and J. C. Davis, Nature **403**, 746 (2000).
[2] E. W. Hudson, K. M. Lang, V. Madhavan, S. H. Pan, H. Eisaki, S. Uchida, and J. C. Davis, Nature **411**, 920 (2001).
[3] E. W. Hudson, V. Madhavan, K. McElroy, J. E. Hoffman, K. M. Lang, H. Eisaki, S. Uchida, and J. C. Davis, Physica B **329-333**, 1365 (2003).
[4] M. E. Flatté, Phys. Rev. B **61**, R14920 (2000).
[5] A. Polkovnikov, S. Sachdev, and M. Vojta, Phys. Rev. Lett. **86**, 296 (2001).
[6] J.-X. Zhu and C. S. Ting, Phys. Rev. B **64**, 060501 (2001).
[7] I. Martin, A. V. Balatsky, and J. Zaanen, Phys. Rev. Lett. **88**, 097003 (2002).

[8] J.-M. Tang and M. E. Flatté, Phys. Rev. B **66**, 060504(R) (2002).
[9] G. V. M. Williams and S. Krämer, Phys. Rev. B **64**, 104506 (2001).
[10] A. Shnirman, I. Adagideli, P. M. Goldbart, and A. Yazdani, Phys. Rev. B **60**, 7517 (1999).
[11] M. E. Flatté and J. M. Byers, in *Solid State Physics*, edited by H. Ehrenreich and F. Spaepen (Academic Press, New York, 1999), vol. 52, pp. 137–228.
[12] M. E. Flatté and J. M. Byers, Phys. Rev. B **56**, 11213 (1997).
[13] M. R. Norman, M. Randeria, H. Ding, and J. C. Campuzano, Phys. Rev. B **52**, 615 (1995).
[14] S. H. Pan, J. P. O'Neal, R. L. Badzey, C. Chamon, H. Ding, J. R. Engelbrecht, Z. Wang, H. Eisaki, S. Uchida, A. K. Gupta, K.-W. Ng, E. W. Hudson, K. M. Lang, J. C. Davis, Nature **413**, 282 (2001).
[15] The STM data for Zn impurities can also be fitted using $V_0 = -85$ meV and $V_1 = 60$ meV, and the other parameters are the same.
[16] M. E. Flatté and J. M. Byers, Phys. Rev. Lett. **80**, 4546 (1998).
[17] J. L. Tallon, J. W. Loram, and G. V. M. Williams, Phys. Rev. Lett. **88**, 059701 (2002).
[18] J. Bobroff, H. Alloul, W. A. MacFarlane, P. Mendels, N. Blanchard, G. Collin, and J.-F. Marucco, Phys. Rev. Lett. **86**, 4116 (2001).